

## PEG prodrug of gambogic acid: Amino acid and dipeptide spacer effects

Ya Ding<sup>a,b</sup>, Peng Zhang<sup>b</sup>, Xiao-Yan Tang<sup>b</sup>, Can Zhang<sup>a,b,\*</sup>, Song Ding<sup>b</sup>, Hai Ye<sup>b</sup>, Qi-Long Ding<sup>b</sup>, Wen-Bin Shen<sup>c</sup>, Qi-Neng Ping<sup>b</sup>

<sup>a</sup>State Key Laboratory of Natural Medicines, China Pharmaceutical University, Nanjing 210009, PR China

<sup>b</sup>School of Pharmacy, China Pharmaceutical University, Nanjing 210009, China

<sup>c</sup>Center for Instrumental Analysis, China Pharmaceutical University, Nanjing 210009, China

### ARTICLE INFO

#### Article history:

Received 8 December 2011

Received in revised form

20 January 2012

Accepted 16 February 2012

Available online 24 February 2012

#### Keywords:

Polymeric prodrug

Gambogic acid

Poly(ethylene glycol)

### ABSTRACT

The clinical application of gambogic acid (GA), a natural component with promising antitumor activity, was limited due to its extremely poor aqueous solubility, rapid elimination in vivo, and wide bio-distribution. To solve these problems, 30 poly(ethylene glycol)-amino acid (or dipeptide)-gambogic acid (PEG-spacer-GA) conjugates were synthesized. All polymeric prodrugs showed satisfactory aqueous solubility ( $1.2 \times 10^3$ – $4.5 \times 10^5$  times of GA solubility). It was found that the molecular weight of PEG and the choice of spacers played important role in controlling the drug percentage, water solubility, and drug release properties of PEG-GA conjugates with and without spacers. Studies of pharmacokinetics, bio-distribution, and cell cytotoxicity revealed that, employing the polymeric conjugation strategy, the remarkably improved circulatory retention time and bioavailability, as well as reduced peripheral toxicity were obtained in comprising with GA and its Cremophor EL formulation. The liver target character of PEG-GA conjugates made them potential prodrugs for liver cancer treatment.

© 2012 Elsevier Ltd. All rights reserved.

### 1. Introduction

In the past decades, polymeric prodrug strategy has been employed to solve practical application problems of many hydrophobic anticancer drugs such as Paclitaxel, Doxorubicin and Camptothecin [1]. Conjugating drug molecules with biocompatible water-soluble polymers, e.g. poly(ethylene glycol) (PEG), will increase water solubility of lipophilic drugs, extend the half-life ( $t_{1/2}$ ) of most drugs, accumulate in the tumor via the enhanced permeability and retention (EPR) effect, and produce enhanced therapy efficacy [2,3].

Gambogic acid (GA, shown in Fig. 1) is the major active ingredient of gamboge [4,5], a brownish to orange resin obtained from various *Garcinia* species. It has been revealed in 1970s that, by selectively inducing apoptosis in tumor cells, GA exhibited extensive and potential anti-tumor activities both in vitro and in vivo [6,7], without significant inhibitory effect on the hemopoietic and immune functions. However, the main obstacles for GA in clinical applications are due to its extremely poor aqueous solubility (less

than 0.5  $\mu\text{g/mL}$ ), rapid plasma clearance, and wide distribution in vivo [8,9], which would cause low bioavailability.

To solve these problems, the introduction of solubilizers, such as L-arginine or Cremophor EL, has been employed to improve the water solubility of GA [10,11]. However, these agents may cause a series of side-effects such as hypersensitivity reactions, nephrotoxicity, neurotoxicity, and cardiotoxicity. And rapid plasma elimination of GA cannot be avoided by these formulations [12].

The utility of polymeric carriers is an alternative way to solve the problem. In our previous work, GA was encapsulated in micelle, which was constructed by amphipathic chitosan derivatives (N-octyl-O-sulfate chitosan, NOSC) [13,14]. Comparing with GA-L-arginine formulation, NOSC-encapsulated drug showed higher drug-loading rate ( $29.8 \pm 0.17\%$ ) and improved entrapment efficiency ( $63.8 \pm 0.52\%$ ). Additionally, in the experiment in vivo, the increased area under concentration–time curve (AUC), prolonged elimination half-life ( $t_{1/2\beta}$ ), passive liver target, and low nephrotoxicity were also achieved.

However, unlike these self-assembled nanovehicles such as micelles that tend to dissociate and release encapsulated drug upon intravenous administration, polymeric prodrugs are much more stable and may effectively prevent premature drug release. In the polymeric prodrug family, PEG prodrugs have received tremendous interest for targeted cancer therapy, due to the unique biocompatible and water-soluble properties of PEG polymer [15–17],

\* Corresponding author. State Key Laboratory of Natural Medicines, China Pharmaceutical University, Nanjing 210009, PR China. Fax: +86 025 8327 1171.

E-mail address: [zhangcan@cpu.edu.cn](mailto:zhangcan@cpu.edu.cn) (C. Zhang).

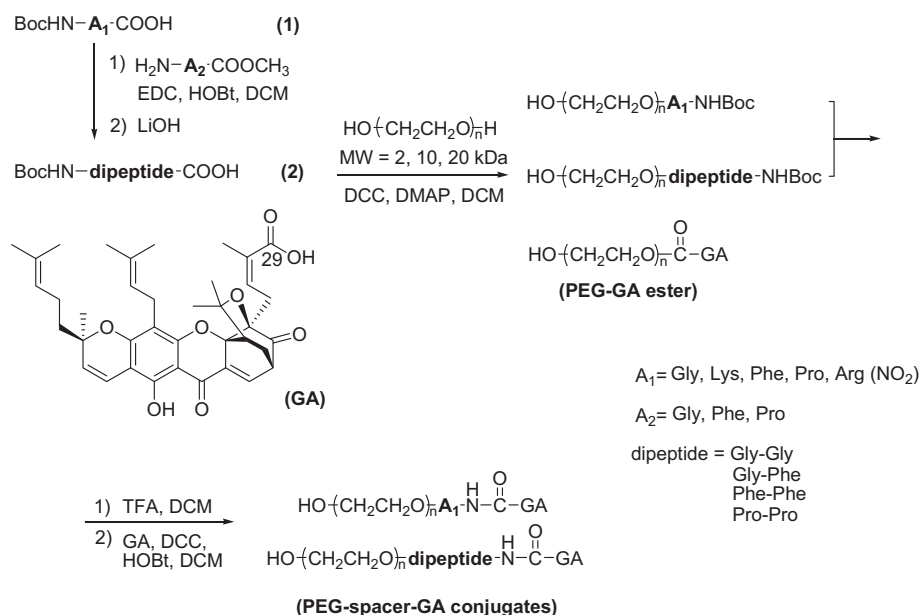


Fig. 1. Chemical structure of GA and synthetic scheme of PEG–GA conjugates with and without amino acid or dipeptide spacers.

which has been approved by FDA. A variety of PEG–drug conjugates [3,18,19], including protein, peptide, and several chemotherapy agents [20–23], such as doxorubicin, paclitaxel, gemcitabine, and camptothecin, have been reported.

In addition to the choice of polymeric partial, polymer linkage is an important factor in determining therapeutic potentials. The connection between PEG and drug can be a direct chemical bond [20–23], including hydrazone, ester, and amide bonds, or be a heterobifunctional spacer such as amino acid based linkages [22,24–26]. Glycine, alanine, and small peptides are preferred due to their chemical versatility for covalent conjugation and biodegradability, which can be a specific substrate for plasmin enzyme whose concentration is high in various kinds of tumor mass [24,26].

In this work, for improving water-solubility, circulation time in body, and pharmacokinetic profiles of GA, 30 PEG–GA conjugates linked with and without spacers (including 5 amino acids and 4 dipeptides) were synthesized. The in vitro drug release, pharmacokinetics, biodistribution, and cell cytotoxicity of PEG–GA conjugates were systematically investigated to demonstrate the importance of molecular weight of polymer and steric hindrance of spacers in the design of macromolecular prodrugs.

## 2. Experimental details

### 2.1. Materials

PEG with molecular weight (MW) of 2, 10, and 20 kDa was purchased from Sinopharm Chemical Reagent Co. (Shanghai, China). All amino acids and their esters were purchased from GL Biochem Ltd. (Shanghai, China), and gamboge resin was obtained from Anhui Bozhou Herb Market (Anhui, China). HPLC grade reagents were used in HPLC analysis, and other reagents were analytical grade and used as received. Deionized water (>18 M $\Omega$ , Purelab Classic Corp., USA) was used in all experiments.

### 2.2. Measurements

$^1\text{H}$  NMR spectra were determined on a Bruker (AVACE) AV-500 spectrometer using deuterated chloroform as the solvent. UV/Vis spectra were recorded on a UV-2401 PC UV/Vis spectrophotometer

(Shimadzu, USA). HPLC was performed using an Agilent 1100 series with a Diamonsil<sup>®</sup> C18 reversed-phase chromatography column (250  $\times$  4.6 mm) and the detection wavelength was 360 nm. Methanol/water (93/7, v/v, pH 3.5) solution acidified by phosphoric acid was used as the mobile phase, and the flow rate was set to be 1 mL/min.

### 2.3. General synthesis method of PEG-spacer-GA conjugates

#### 2.3.1. Isolation and purification of gambogic acid

Dry gamboge resin from the *Garcinia hanburyi* tree (100 g) was suspended in pyridine (300 mL) and stirred at 80–90  $^\circ\text{C}$  for 30 min to form a pyridine salt of GA. After filtered through kieselguhr, 20 mL water was added into the filtrate. The mixture was cooled to 4  $^\circ\text{C}$  overnight, and the precipitate was collected and washed with pyridine solution (70%, v/v) and water for several times. After dried under reduced pressure, a yellow powder was dissolved in ethyl ether (500 mL) to reflux for 30 min, and then filtrated, concentrated and precipitated by using petroleum ether, the yellow precipitate of GA pyridine salt was collected and dried. The obtained solid was dissolved in ethyl ether (250 mL) and washed with aqueous HCl (1 M) and water. The ether solution was then dried over sodium sulfate and evaporated to yield an orange powder of 8.2 g (GA, purity 96.7%, w/w, analyzed by HPLC).

A general synthesis method was followed for obtaining all PEG–GA conjugates (showed in Fig. 1), and synthesis procedure of PEG<sub>2kDa</sub>–pro–pro–GA conjugate was described as an example.

#### 2.3.2. *N*-tert-butoxycarbonyl-prolyl-proline methyl ester (Boc–pro–pro–COCH<sub>3</sub>)

The synthesis of compounds **1**, *N*-tert-butoxycarbonyl-amino acid, was referred to a previous report [27]. The resultant *N*-tert-butoxycarbonyl-L-proline (2.15 g, 0.01 mol) was dissolved in dichloromethane (DCM, 10 mL). Slow dropping of HOBT (1.62 g, 0.012 mol) in a minimal amount of tetrahydrofuran (THF) was over 30 min. When the solution was cooled to 0  $^\circ\text{C}$ , EDC hydrochloride (2.11 g, 0.011 mol) in DCM (15 mL) was added, and additional stir for 30 min in ice-water bath was carried out. And then, a well-mixed DCM solution (20 mL) containing L-proline methyl ester hydrochloride (1.82 g, 0.011 mol) and 4.5 mL triethylamine (TEA, 0.033 mol) was added into the reaction solution and stirred at room

temperature overnight. After evaporation under reduced pressure, the residue was suspended in ethyl acetate and filtrated. The filtrate was washed with dilute citric acid, saturated sodium bicarbonate solution, and water. Dried over anhydrous sodium sulfate and concentrated in vacuum, the off-white Boc–pro–pro–COCH<sub>3</sub> was obtained (2.83 g, 87%).

### 2.3.3. *N*-tert-butoxycarbonyl-prolyl-proline (Boc–pro–pro–COOH)

After Boc–pro–pro–COCH<sub>3</sub> (1.5 g, 4.6 mmol) was dissolved in methanol (15 mL) and cooled to 0 °C, 7 ml of LiOH aqueous solution (7 mmol) was added dropwise into the solution to react for 1 h at 0 °C and 2 h at room temperature. After reaction, methanol was removed from the solution by evaporation. The resultant aqueous phase became turbid when pH value was adjusted to ~3 with potassium hydrogen sulfate (1 mol/L) at 0 °C. Extracted by ethyl acetate for three times, the organic layer was washed with saturated sodium chloride solution, dried over sodium sulfate, and evaporated to yield white powder, Boc–pro–pro–COOH (1.1 g, 77%).

### 2.3.4. Boc–pro–pro–PEG<sub>2kDa</sub>

PEG (2.0 g, 2 mmol OH, MW = 2 kDa), Boc–pro–pro–COOH (0.9 g, 3 mmol), and DMAP (0.07 g, 0.6 mmol) were dissolved in anhydrous DCM (30 mL), and DCC (0.66 g, 3.2 mmol) was added into the solution and stirred overnight. Produced dicyclohexylurea (DCU) was filtered off and DCM in filtrate was evaporated. The residue was dissolved in ethyl acetate and cooled at 4 °C to filter trace DCU. The filtrate was concentrated to a mud-like sample, which was added dropwise to 100 mL of vigorously stirred cold ethyl ether. The white precipitate was filtered and dried under reduced pressure, affording the crude product of Boc–pro–pro–PEG<sub>2kDa</sub> (1.8 g, 90%) used without further purification.

### 2.3.5. PEG<sub>2kDa</sub>–pro–pro–NH<sub>2</sub>

The crude product of Boc–pro–pro–PEG<sub>2kDa</sub> (1.8 g) was dissolved in 10 mL of TFA/DCM (1:1, v/v) and stirred at 0 °C for 1 h. When deprotection process was completed, the solvent was removed under reduced pressure, and the resulting slurry was added dropwise to vigorously stirred cold ethyl ether. The precipitate was collected and resolved in ethanol/ethyl ether mixed solvent to make a saturated solution, and the mixture solution was then cooled to form a white precipitate. The solid was washed with ethyl ether for several times, and the white powder was dried in a vacuum overnight to obtain PEG<sub>2kDa</sub>–pro–pro–NH<sub>2</sub> (1.45 g, 81%).

### 2.3.6. PEG<sub>2kDa</sub>–pro–pro–GA conjugate

GA (0.75 g, 1.2 mmol), PEG<sub>2kDa</sub>–pro–pro–NH<sub>2</sub> (1.2 g, 1 mmol) in anhydrous DCM (15 mL), and HOBt (0.19 g, 1.4 mmol) in a minimal amount of THF were mixed at room temperature. A solution of DCC (0.29 g, 1.4 mmol) in a minimal amount of DCM was added and the reaction solution was stirred for 24 h. After filtration and evaporation, an oily substance was obtained and resolved in isopropanol to make a saturated solution, and the solution was then cooled to form an orange precipitate. The orange powder was filtered, washed with ether and dried in a vacuum to afford PEG<sub>2kDa</sub>–pro–pro–GA conjugate (0.97 g, 81%).

### 2.3.7. PEG<sub>2kDa</sub>–GA ester

PEG<sub>2kDa</sub>–GA ester without spacers was prepared in a similar fashion to the above procedure, where PEG<sub>2kDa</sub> (1 equiv.) and GA (2 equiv.) were directly coupled utilizing the DCC/HOBt method in 82% (w/w) yield. The same procedure could also be used for the synthesis of PEG<sub>10kDa</sub>– and PEG<sub>20kDa</sub>–GA esters.

## 2.4. Drug content of PEG–GA conjugates

An ultraviolet absorbance method at a fixed wavelength (360 nm), where PEG and spacer have no absorption, was established for the determination of GA content in PEG–GA conjugates. The GA content of conjugates was determined with the help of a calibration curve of GA in methanol, range from 2 to 40 µg·mL with  $R^2 = 0.9991$ , and the GA content was calculated as follows:

$$\text{GA\%} = \left( \frac{m_{\text{GA}}}{m_{\text{prodrug}}} \right) \times 100\%$$

## 2.5. Solubility of PEG–GA conjugates

A visual observation method was used to evaluate the solubility of PEG–GA conjugates. An exact amount of sample (100 mg) was weighed and placed in a volumetric flask (2 mL) and 25 µL aliquots of distilled water were added sequentially using a pipette, followed by sonication for 30 s. When the solution became fluidic and clear, the total volume of water added was calculated. The experiment was carried out at 25 °C, and each sample was repeated in triplicate.

## 2.6. In vitro drug release of PEG–GA conjugates

In vitro GA release from the conjugates was performed by both chemical and enzymatic hydrolysis.

The chemical hydrolysis was carried out in triplicates in PBS at pH 7.4 and 5.5 at 37 °C, respectively. The solution (10 mL) of all conjugates of 10 mmol equivalent GA concentration was stirred mildly. At the scheduled time, 20 µL of the solution was analyzed by an HPLC method to determine the release of GA from conjugates ( $t_{R, \text{prodrug}} = 2.67$  min and  $t_{R, \text{GA}} = 14.48$  min). The half-life of each conjugate in different media was calculated using linear regression analysis.

The method for analysis of GA release in plasma and in liver homogenate was similar to that of hydrolysis in PBS, except for the pretreatment process. Blank human plasma was procured from the Nanjing Red Cross Blood Center. Rat liver tissue was accurately weighed (300–500 mg) and homogenized in 2.5 mL of normal saline containing 1.9% w/v NaCl (Sodium Chloride) solution prior to use. PEG–GA conjugate (100 mmol GA equivalent content) in 100 µL of saline was added to 10 mL of plasma/liver homogenate and incubated at 37 °C with mild stirring. At designated time intervals, 150 µL of plasma or liver homogenate solution was treated with 50 µL of 1 M hydrochloric acid and extracted by 800 µL of acetonitrile on a vortex mixer for about 3 min followed by centrifugation at 10,000 rpm for 10 min. The clear supernatant liquid was analyzed by an HPLC method and the half-life of each sample was calculated accordingly. Each experiment was repeated in triplicate.

## 2.7. In vivo pharmacokinetics

The animal experiment protocols were approved by the University Ethics Committee for the use of experimental animals and conformed to the Guide for Care and Use of Laboratory Animals. The in vivo pharmacokinetics was carried out in Sprague–Dawley rats of 190–220 g and 4–6 weeks old. The rats were supplied by the Laboratory Animal Center of Nantong University. The animals were held in air-conditioned rooms, provided with standard food and filtered water.

PEG<sub>10kDa</sub>–GA conjugates and a Cremophor EL preparation of GA (GA–C) were diluted in normal saline containing 1.9% w/v NaCl and filtrated through 0.22 µm pore-sized micropore films. Animals were divided into eleven groups with each of five rats and were

given an intravenous injection via tail vein of GA–C, PEG<sub>10kDa</sub>–GA conjugates with and without spacers solution at equivalent dose (4 mg/kg of GA), respectively. All animals were observed for mortality, general condition and potential clinical signs.

The blood samples were collected into the heparinized tube at time period of 0, 5, 15, 30, 60, 90, 120, 180, and 240 min post-treatment. The blood samples were centrifuged at 4000 rpm for 10 min and the separated plasma was stored at –20 °C until analysis. Liquid–liquid extraction was performed by mixing the plasma (150  $\mu$ L) with 50  $\mu$ L of 1 M hydrochloride acid and extracted by 300  $\mu$ L of acetonitrile on a vortex mixer for about 3 min followed by centrifugation at 10,000 rpm for 10 min, after which the upper supernatant was analyzed by using the standard curve-based HPLC method. The parameters of the pharmacokinetics were calculated by using DAS procedures.

### 2.8. Biodistribution

Sprague–Dawley rats (50% male and 50% female) were randomly assigned to four groups ( $n = 100$ ) with intravenous injection of GA–C, PEG<sub>10kDa</sub>–Phe–GA, PEG<sub>10kDa</sub>–Phe–Phe–GA, and PEG<sub>10kDa</sub>–GA conjugate at the equivalent 4 mg/kg dose respectively. Each group has five sets of five rats sacrificed at five designated time points for the biodistribution investigation. Before drug administration, GA–C, PEG<sub>10kDa</sub>–Phe–GA, PEG<sub>10kDa</sub>–Phe–Phe–GA, and PEG<sub>10kDa</sub>–GA conjugate were diluted in normal saline containing 1.9% w/v NaCl and filtrated through 0.22  $\mu$ m pore-sized micropore films to obtain an estimated injection volume of 1–1.5 mL.

Intravenous injection was given via the tail vein. All animals were observed for mortality, general condition and potential clinical signs. Animals in each set were sacrificed by cardiac stick exsanguinations at 5, 30, 60, 120, 240 min, respectively after the injection and tissues (heart, liver, spleen, lung, kidney, and brain) were collected. The tissues were then washed with saline, weighed and homogenized. After that, 1 ml of plasma, an average weight of organ (liver = 0.9140 g, lung = 0.1109 g, heart = 0.0810 g, spleen = 0.1245 g, kidney = 0.2302 g, and brain = 0.3555 g) for each was mixed with PBS, followed by extraction and analysis as the blood sample was done.

### 2.9. Cell cytotoxicity assay

In vitro cytotoxicity of the conjugates was quantified by measuring its IC<sub>50</sub> (drug concentration inhibiting 50% of cells) on a human hepatoma cell strains (HepG2). HepG2 cells were cultured in RPMI-1640 containing heat-inactivated FCS (RPMI-10% FCS) at a density of  $1 \times 10^5$  cells/180  $\mu$ L/well into 96-well microtiter plates and allowed to proliferate at 37 °C in a humidified incubator with 5% CO<sub>2</sub> for 24 h. A total of 20  $\mu$ L serial dilutions of the tested compounds (final GA equivalent concentration 0.5–5000  $\mu$ g/mL, GA was dissolved by DMSO (<1%)) were added to the wells and all samples were prepared and measured in quintuplicate for each concentration. After 24 h of incubation, 20 mL of MTT (5 mg/mL) per well was added and the plates were incubated for a further 4 h. Then, the supernatant was removed followed by the addition of 150  $\mu$ L of DMSO to each well. 15 min after that, the absorbance at 490 nm was detected with a microplate reader and the IC<sub>50</sub> values for each compound were calculated from absorbance vs. dilution factor plots.

## 3. Results and discussion

### 3.1. Synthesis and characterization of PEG–GA conjugates

It has been reported that the 29-carboxy group is a potential structure modification site of GA, [16], which was chosen as the

reaction site for the polymeric conjugation. In our initial synthesis, connecting GA with spacer firstly showed a relatively higher binding efficiency of drug with spacer molecules. However, GA was found to be unstable in the conjugation and after treatment processes, due to the instability of the  $\alpha$ ,  $\beta$ -unsaturated ketone at the C-10 position [28,29]. Therefore, the synthesis of PEG–spacer and then the coupling of GA on polymer were proceeded as shown in Fig. 1.

t-Boc-protected amino acids (1, including Gly, Lys, Phe, Pro, and Arg(NO<sub>2</sub>)) was synthesized firstly to act as the amino acid spacer in PEG–GA conjugate preparation. Coupling t-Boc-protected Gly, Phe, and Pro with their corresponding methyl esters would lead to t-Boc-dipeptide methyl esters (dipeptide = Gly–Gly, Gly–Phe, Phe–Phe, and Pro–Pro). And then, t-Boc-dipeptide (2), for connecting PEG and GA as the dipeptide spacer, can be obtained by careful hydrolysis with lithium hydroxide to release free carboxyl group of dipeptide.

Conjugating PEG molecule (MW = 2, 10, and 20 kDa) with GA and t-Boc-spacer (1 or 2), respectively, PEG–GA esters and t-Boc-spacer-PEG conjugates were obtained. The removal of the t-Boc moiety on amino acid or dipeptide spacer was achieved with acid treatment (TFA/DCM) in an ice bath. Finally, the classical DCC/HOBt catalyzed coupling of PEG–spacer–NH<sub>2</sub> and GA was carried out to yield the crude product of PEG–spacer–GA conjugates. All conjugates were resolved in 2-propanol to form a saturated solution, and the solution was cooled to obtain yellow solid and wash with ethyl ether for several times, the un-reacted GA and other undesired substances were separated from the conjugates.

All of final conjugates were characterized by FT-IR and <sup>1</sup>H NMR analysis in CDCl<sub>3</sub> [30]. For instance, the typical FT–IR spectra of PEG<sub>2kDa</sub> and PEG<sub>2kDa</sub>–Pro–Pro–GA conjugate were shown in Fig. 2 (A and B, respectively). In the spectrum of PEG<sub>2kDa</sub>, the absorption bands located at 2860 cm<sup>–1</sup> and 1464 cm<sup>–1</sup> are, respectively, due to the adsorption of C–H stretching and bending vibrations of methylene groups in PEG. The broad band at 3346 cm<sup>–1</sup> arises from O–H stretching vibration of hydroxyl ends on PEG, and the absorbance of 1110 cm<sup>–1</sup> is due to C–O stretching vibration in PEG backbone. While several new IR signals attributed to the Pro–Pro spacer and GA structure are shown in IR spectrum of PEG<sub>2kDa</sub>–Pro–Pro–GA conjugate in Fig. 2 (curve B) in comparison with that of PEG<sub>2kDa</sub>. The absorption band at 1739 cm<sup>–1</sup> can be assigned to  $\nu_{C=O}$  in ester bond between GA and Pro–Pro spacer. And new absorbance peaks located at 1653 cm<sup>–1</sup> and 1626 cm<sup>–1</sup>/1593 cm<sup>–1</sup> attributed to  $\nu_{C=O}$  of amide I group and  $\nu_{C=C}$  of benzene

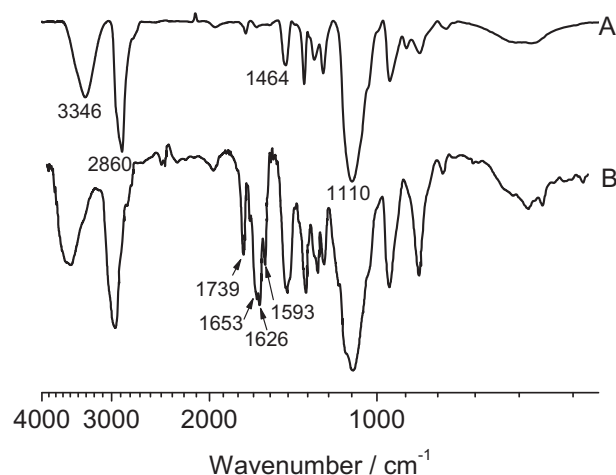


Fig. 2. FT–IR spectra of PEG<sub>2kDa</sub> (curve A) and PEG<sub>2kDa</sub>–Pro–Pro–GA conjugate (curve B).

ring, respectively, indicate the successful linkage of dipeptide spacer and conjugation of GA molecule on PEG long chain.

$^1\text{H}$  NMR spectra of PEG-GA and PEG-Pro-Pro-GA conjugate were shown in Fig. 3 (PEG MW = 2 kDa). Resonance at 3.7 ppm corresponding to protons on PEG appeared in both spectra, in which characteristic peaks of GA were also showed. It displayed the existence of PEG and GA in conjugate regardless of the spacer. By comparison of the resonances associated with PEG-pro-pro-GA conjugate with those associated with PEG-GA ester, additional chemical shifts at ca. 4.5, 3.5, and 2.1 ppm (marked with stars in Fig. 3) can be attributed to protons in Pro-Pro spacer. It demonstrated the successful linkage of dipeptide spacer between PEG and GA molecules.

### 3.2. Drug content of PEG-GA conjugates

Fig. 4 showed the GA content in all PEG-GA conjugates. It was found that with PEG MW rose from 2 to 20 kDa, GA content of conjugates decreased obviously. GA content in PEG-GA esters decreased from 22.09 to 0.49, and the average value of spacer-linked conjugates dropped from 20.82 to 3.17, respectively. This phenomenon could be due to two reasons, the GA content calculation method and the steric hindrance of PEG polymers. Due to the calculation method,  $\text{GA}\% = (m_{\text{GA}}/m_{\text{prodrug}}) \times 100\%$ , large polymeric molecular weight leading to low theoretical GA content value was reasonable. However, comparing the theoretical and measured values of conjugates, several PEG<sub>2kDa</sub>-based conjugates showed higher GA content than their theoretical values (Fig. 4, curve A<sub>0</sub> and A). However, measured GA content of PEG<sub>20kDa</sub>-based conjugates (curve C) was relatively consistent with their theoretical value (curve C<sub>0</sub>). This result indicated the existence of disubstituted GA-

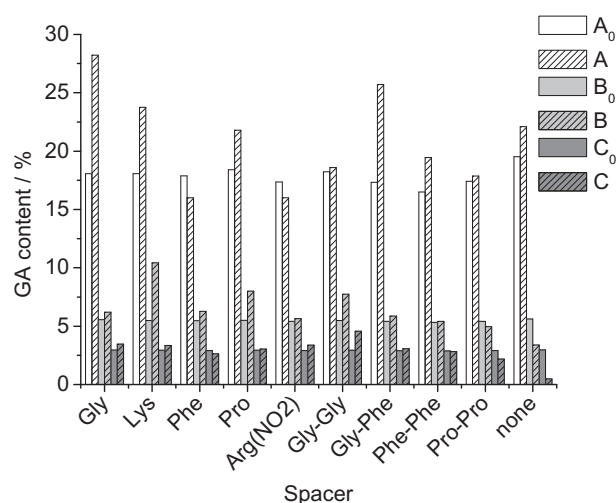


Fig. 4. The theoretical (A<sub>0</sub>–C<sub>0</sub>) and measured (A–C) values of GA content in PEG-GA conjugates with and without different spacers (PEG MW = 2 (A<sub>0</sub> and A), 10 (B<sub>0</sub> and B), and 20 (C<sub>0</sub> and C) kDa).

PEG-GA molecules in low molecular weighted PEG<sub>2kDa</sub> conjugates, and that high PEG MW products (PEG<sub>20kDa</sub>-GA prodrugs) were more inclined to be the mono-substituted compound. It implied that the terminal concentration became lower with increasing MW of PEG, which would depress the efficiency of conjugation reaction.

In addition, keeping PEG MW unchanged, it was found that the existence and selection of amino acid or dipeptide spacers played

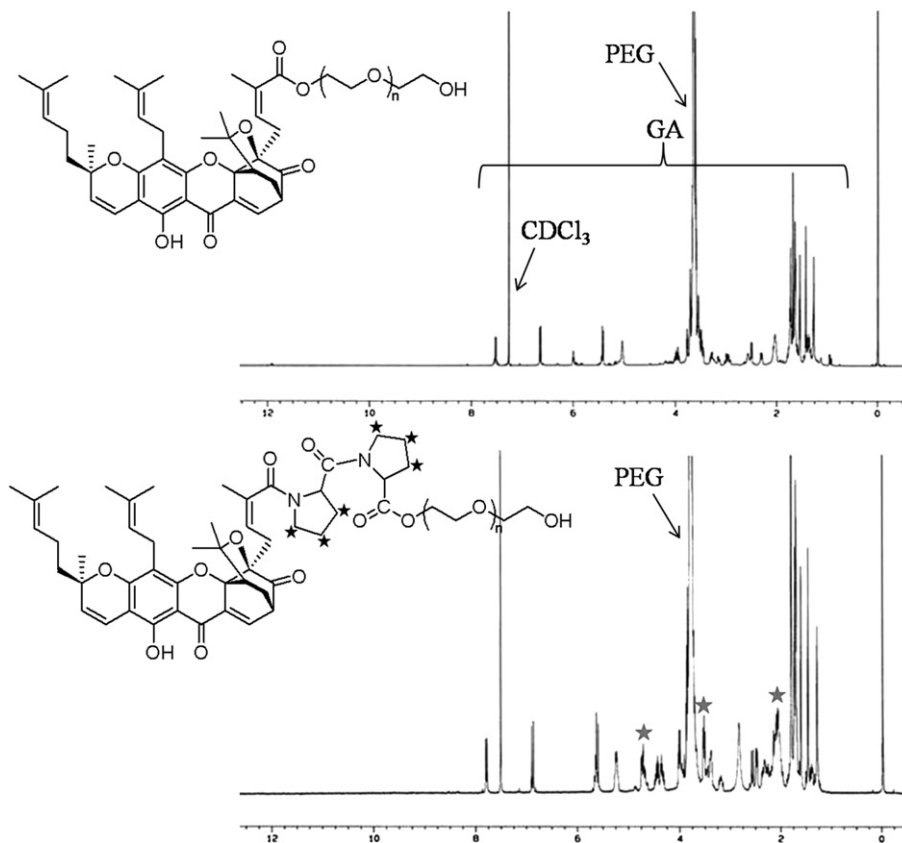


Fig. 3.  $^1\text{H}$  NMR spectra of PEG<sub>2kDa</sub>-GA ester and PEG<sub>2kDa</sub>-Pro-Pro-GA conjugate.

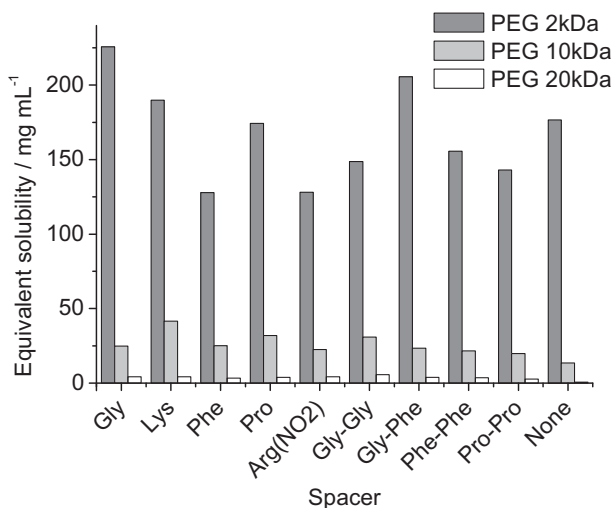


Fig. 5. Equivalent aqueous solubility of GA in conjugates.

an important role in adjusting GA content results. On one hand, the GA percentage of PEG-GA ester always showed lower value than that of conjugate containing spacers, especially in cases of large polymer prodrugs (Fig. 4, curves B and C). It indicated that, in comprising with hydroxyl-terminated PEG, amino acid or dipeptide-modified PEG molecules can be seen as an activated polymer, which showed higher conjugation efficiency with drugs. On the other hand, those spacers having large side chain groups, such as Arg(NO<sub>2</sub>), Phe, and Pro, would result in low GA percentage no matter how much the PEG MW was.

### 3.3. Solubility of PEG-GA conjugates

A direct observation method is used to evaluate the solubility of PEG-GA conjugates [31], and the equivalent solubility value was calculated depending on the measured solubility and GA content in Fig. 4. Compared with the extremely poor solubility of parent drug (GA, 0.5 μg·mL<sup>-1</sup>), all of conjugates exhibited satisfactory aqueous solubility, which was 1.2 × 10<sup>3</sup>-fold (PEG<sub>20kDa</sub>-GA, 0.61 mg·mL<sup>-1</sup>) at least and 4.5 × 10<sup>5</sup>-fold (PEG<sub>2kDa</sub>-Gly-GA, 225.6 mg·mL<sup>-1</sup>) at most of GA (shown in Fig. 5).

Although there was disubstituted GA on both ends of PEG in the case of PEG<sub>2kDa</sub>-based prodrugs, PEG<sub>2kDa</sub>-GA conjugates still showed the best water solubility due to the best aqueous solubility of PEG<sub>2kDa</sub> and the possibility of micellar formation self-assembled by PEG<sub>2kDa</sub>-GA conjugates in the aqueous solution. It suggested that the solubility of prodrugs was highly depended on the water solubility of polymer used.

Comparing with PEG-GA esters having the same PEG MW, the existence of spacers had little effect in enhancing the water solubility of conjugates in the case of PEG<sub>2kDa</sub>-spacer-GA sample. However, PEG<sub>10kDa</sub>- and PEG<sub>20kDa</sub>-spacer-GA samples displayed better aqueous solubility than those of their esters, although it showed no obvious regularity among different spacers. It implied that the function of spacer in controlling the polymer prodrug properties was generally reflected in large MW cases, which was consistent with the result of GA content.

### 3.4. In vitro drug release of PEG-GA conjugates

Considering the possible in vivo process of prodrugs, chemical and enzymatic hydrolysis was carried out to evaluate the drug release behavior of PEG-GA conjugates by using HPLC method. The half-life (*t*<sub>1/2</sub>) values corresponding to all conjugates and hydrolysis

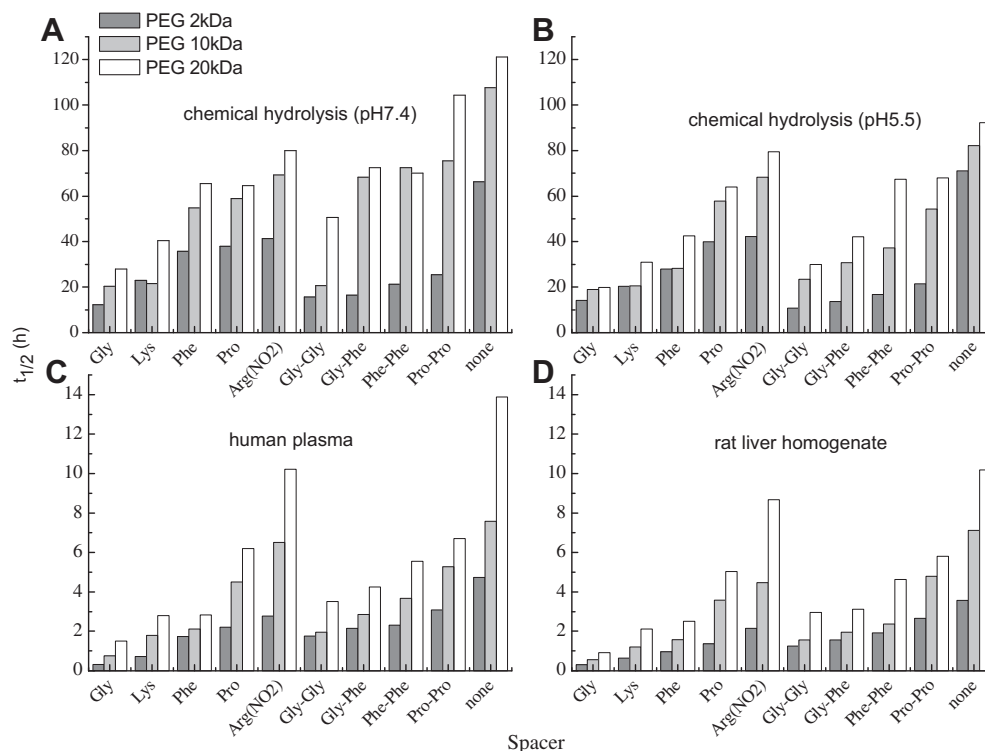


Fig. 6. In vitro drug release: half life of each conjugate in various media at 37 °C toward chemical hydrolysis and enzymolysis in (A) buffer pH 7.4, (B) buffer pH 5.5, (C) human plasma, and (D) rat liver homogenate (All experiments were done in triplicate. SD = ±10%).

conditions were shown in Fig. 6. The results implied several important clues, demonstrating the structure-dependent properties of conjugates in this work.

Firstly, PEG–GA esters, connecting GA and PEG molecules with ester bond directly, displayed the highest stability towards both chemical and enzymatic hydrolysis. It is consistent with the previous literature [18,19,24], reporting that several PEG–drug esters were excreted in the form of prodrug before exerting its pharmacodynamic effect. In contrast, conjugates with amino acid or dipeptide spacers showed relative fast and appropriate drug release velocity, insuring the effective release of bioactive molecules.

Secondly, the drug release behavior toward chemical hydrolysis was evaluated at pH 7.4 and 5.5 in PBS (37 °C) to mimic the physiological and cell lysosomal environments, respectively (Fig. 5A and B). The  $t_{1/2}$  values for products at pH 5.5 were commonly shorter than those at pH 7.4, implying that lower pH environment led to faster releasing speed. Namely, selective release of active drug (GA in this case) under the acidic physical environment in cancer cells rather than in normal cells could be achieved.

Thirdly, drug release by enzymatic hydrolysis was also tested to evaluate the release properties of conjugates in the presence of nonspecific proteases (in human plasma) or hydroamidases in the liver (in rat liver homogenate) (shown in Fig. 6C and D). It revealed that all conjugates were more rapidly activated to GA in human plasma and rat liver homogenates than in PBS. For example, in PBS at pH 5.5, the half-lives of the PEG–Arg(NO<sub>2</sub>)–GA conjugates with PEG MW of 2, 10, and 20 kDa were 42.2 h, 68.4 h, and 79.5 h, respectively. While in human plasma, 50% of GA was released from the same conjugates after only 2.8 h, 6.5 h, and 10.2 h. And in the liver homogenate, the half-lives were even shorter. These results strongly suggest that enzymatic activation may be the major contributor to the release of GA from the polymeric conjugates in vivo.

Fourthly, increased steric hindrance provided by spacers with large side chain could lead to a significantly prolonged release character under the same environmental condition. In the case of amino acid spacers, the half-life of PEG conjugates employing Arg(NO<sub>2</sub>) or Phe spacer showed at most 8 or 5 times longer  $t_{1/2}$  values than those using Gly moiety. Similarly, for the dipeptide-connected conjugates, such as Gly–Gly, Gly–Phe, and Phe–Phe spacers, a gradually prolonged half-life value was found due to the increasing size of the  $\alpha$ -substituted group in spacers. This can be interpreted that the large side chain-induced steric hindrance would become an obstacle for the enzyme approaching, and lead to a decreased hydrolysis rate and prolonged half-life.

Finally, the molecular weight of PEG is another factor that can contribute to the GA release control. The lower terminal concentration arising from the increasing MW of PEG made the action site of the proton or enzyme inaccessible and slowed down the

hydrolysis rate. As shown in Fig. 6, PEG<sub>20kDa</sub>–GA conjugates were the most stable compounds, of which the half-lives were 2–5 times as those of PEG<sub>2kDa</sub> with the same spacers.

### 3.5. In vivo pharmacokinetics

Conjugates of PEG<sub>10kDa</sub> series were chosen and assayed for in vivo pharmacokinetics. A Cremophor EL preparation of GA (GA–C) was selected as the control. In this study, GA concentrations in plasma was measured over 4 h after the i.v. injection of conjugates or GA–C to rats at a dose of 4 mg/kg (equivalent GA concentration), and the plasma concentration–time curves were analyzed by two-compartment models. The pharmacokinetic parameters were presented Table 1.

Conjugates obviously showed prolonged mean residence time (MRT) and elimination half-life ( $t_{1/2\beta}$ ), in comparison with both GA (MRT = 21.05 min,  $t_{1/2\beta}$  = 16.07 min) [15] and GA–C. This result may attribute to the polymeric protection role of PEG and stable drug

**Table 1**  
Pharmacokinetic study of PEG<sub>10kDa</sub>–GA conjugates ( $n = 5$ ).

Spacer in conjugates	AUC ( $\mu\text{g min/ml}$ )	MRT (min)	$t_{1/2\alpha}$ (min)	$t_{1/2\beta}$ (min)	Vd (ml)	Cl (ml/min)
GA–C	85.41	38.52	9.35	46.03	239.94	11.91
Gly	437.14	39.93	7.23	52.18	54.48	2.28
Lys	516.56	43.44	20.87	85.63	75.94	4.43
Phe	463.79	50.19	16.77	72.91	67.81	3.54
Pro	376.81	49.05	13.29	73.12	59.01	3.23
Arg(NO <sub>2</sub> )	219.82	56.73	19.54	72.19	82.07	4.22
Gly–Gly	381.48	58.73	7.87	48.32	25.25	0.44
Gly–Phe	308.7	69.72	9.26	61.64	12.3	0.61
Phe–Phe	227.18	81.03	17.22	99.27	20.11	1.24
Pro–Pro	239.76	96.31	16.07	161.61	18.83	3.24
None	208.65	57.58	11.55	73.37	89.37	1.22

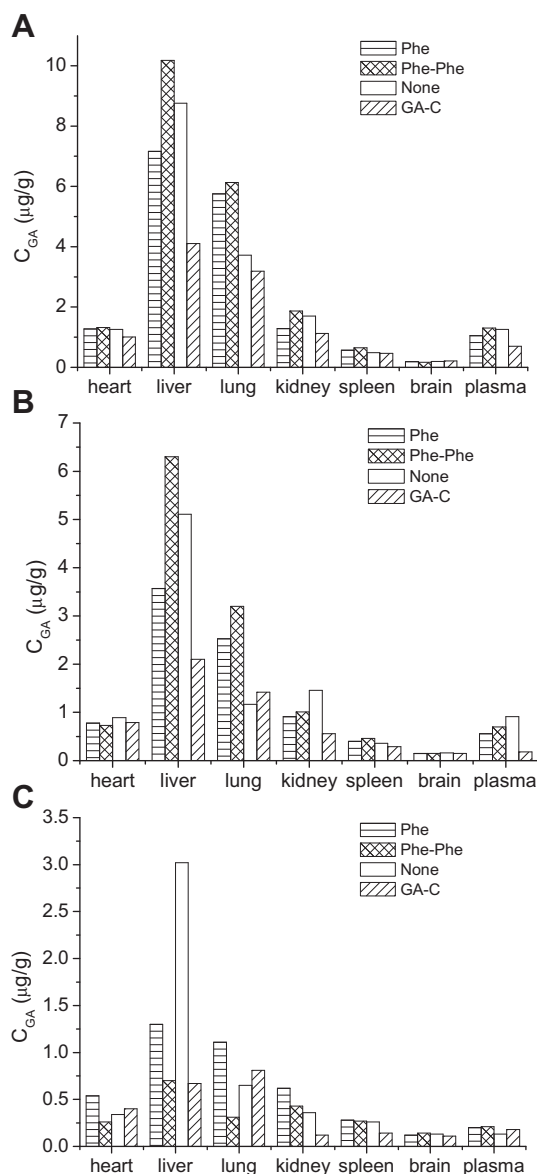


**Fig. 7.** Tissue distribution profile of GA in mice after i.v. administration of PEG<sub>10kDa</sub>–Phe–GA (Phe), PEG<sub>10kDa</sub>–Phe–Phe–GA (Phe–Phe), PEG<sub>10kDa</sub>–GA (None) and GA–C at a dose of 4 mg/kg at (A) 30 min, (B) 60 min and (C) 120 min.

**Table 2**

AUC(0–∞) (μg/mL min or μg/g min) of GA & relative exposure (re) and AUCi(0–∞) (μg/min)<sup>a</sup> in mice plasma and organs after iv administration of PEG-GA conjugates or Cremophor EL preparation (GA–C) at a dose of equivalent GA 4 mg/kg (n = 5).

Organ	GA–C			PEG <sub>10,000</sub> –Phe–GA			PEG <sub>10,000</sub> –Phe–Phe–GA			PEG <sub>10,000</sub> –GA		
	AUC(0–∞)	re	AUCi(0–∞)	AUC(0–∞)	re	AUCi(0–∞)	AUC(0–∞)	re	AUCi(0–∞)	AUC(0–∞)	re	AUCi(0–∞)
Plasma	95.35	1	95.35	138.357	1.45	138.36	137.80	1.45	137.80	152.32	1.60	152.32
Liver	527.56	1	482.19	824.639	1.56	753.72	862.67	1.64	788.48	1062.65	2.01	971.09
Lung	393.72	1	43.66	623.293	1.58	69.12	572.92	1.46	63.54	383.53	0.97	42.53
heart	153.25	1	12.41	177.772	1.16	14.40	144.12	0.94	11.67	158.61	1.04	12.85
Spleen	76.42	1	9.51	111.599	1.46	13.89	116.24	1.52	14.47	103.75	1.36	12.92
Kidney	111.18	1	25.59	204.128	1.83	46.99	221.03	1.99	50.88	217.99	1.96	50.18
Brain	38.74	1	13.77	47.871	1.24	17.01	88.38	2.28	31.42	47.52	1.23	16.89

<sup>a</sup> AUCi(0–∞) = AUC(0–∞) × average volume of plasma or AUC(0–∞) × average weight of organ.

linkage via the covalent bond. In addition, the reduced blood clearance values (Cl) for conjugates demonstrated that the prolonged drug release and prevention of rapid renal filtration in the circulation were achieved. In addition, an obvious increase, 2.5-fold at least and 6-fold at most, of the area under the plasma concentration–time curve (AUC) in contrast with that of GA–C demonstrated a remarkably enhanced bioavailability. From the in vivo pharmacokinetic studies, it can be found that data of apparent distribution volume ( $V_d$ ) sharply reduced, only 5%–37% of the control group value (GA–C). This phenomenon may contribute to a reduction in peripheral toxicity, and implied that the bio-distribution of GA molecule has been changed and governed by the conjugation with the macromolecular carrier. Therefore, bio-distribution studies were carried out to further evaluate the passive target of PEG–GA conjugates.

### 3.6. Biodistribution

Three conjugates (PEG<sub>10kDa</sub>–Phe–GA, PEG<sub>10kDa</sub>–Phe–Phe–GA, and PEG<sub>10kDa</sub>–GA) were selected to test the tissue distribution profiles. The histograms and relative parameters for GA–C, PEG–GA ester, and PEG-spacer–GA conjugates were showed in Fig. 7 and Table 2, respectively. The results demonstrated that, after i.v. administration for 30 min, GA was found in plasma and all organs we detected. And a high GA concentration in liver and lung was shown no matter what the prescription was, which can be due to the accumulation of conjugates in the endothelial system

concentrated in these tissues. The ratio of drug concentration in liver to that in plasma was calculated to be in the range of 6–10, and the spacer shows no obvious influence in this trend of biodistribution.

In the assay duration from 30 to 120 min, GA concentration detected in liver and lung after the administration of PEG conjugates showed twice as high as that of the control group GA–C.

In addition, higher AUC (area under the plasma or organ concentration–time curve) and re values (relative exposure compared with GA–C) showed that, after conjugated to PEG molecule, kidney filtration rate or overall clearance rate of GA were reduced significantly (shown in Table 2). Actually, more than 70% of the in vivo distribution of GA, revealed by the AUCi, was found in liver, which demonstrated a liver-targeting property of the conjugate. Therefore, due to the tissue distribution profile of the polymeric prodrug system, more effective pharmacodynamic action for liver cancer and reduced systemic toxicity of GA may be expected.

It is noted that, after 120 min, the concentration of GA for PEG–GA ester sample remained at most 23-fold higher in liver than plasma. It indicates slow metabolic rate of the ester in vivo and subsequently accumulated in liver.

### 3.7. Cell cytotoxicity assay

The in vitro biological efficacy of PEG-GA conjugates was evaluated against HepG2 cells using the MTT method. Data in Fig. 8 showed that all of conjugates exhibited obvious cytotoxicity against HepG2 cells, indicating polymeric prodrugs did not lose anti-cancer activity of GA. However, compared with native drug (GA, IC<sub>50</sub> = 3.26 μM), the IC<sub>50</sub> values of conjugates (for instance, IC<sub>50</sub> of PEG<sub>10kDa</sub>–Pro–Pro–GA = 117.66 μM) was as high as 36.1 times that of GA. It suggested a relatively lower cellular cytotoxicity induced by the polymeric derivatization of the excellent biocompatibility of PEG, amino acids, and dipeptide molecules. The cell cytotoxicity was mainly due to the native GA released from the PEGylated conjugates.

## 4. Conclusions

A series of PEG conjugates of the natural antitumor agent gambogic acid with different amino acid and dipeptide spacers was prepared. These PEG-GA conjugates showed satisfactory water solubility compared with gambogic acid. Based on the results in vitro, the molecular weight of polymeric carrier and the choice of spacers had important influence in the solubility, drug content, and drug release behavior of polymeric prodrugs. Moreover, in vivo studies revealed that, employing the polymeric conjugation strategy, the circulatory retention time, biodistribution, and bioavailability of conjugates were remarkably improved, and liver targeting character has been achieved. These results demonstrate

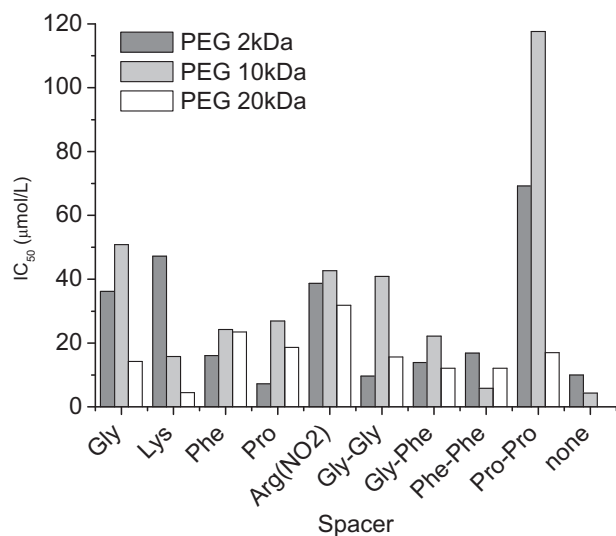


**Fig. 8.** In vitro cytotoxicity of PEGylated conjugates of GA<sup>a</sup> against HepG2 cell lines after 24 h incubation (IC<sub>50</sub>, μmol/L). <sup>a</sup>IC<sub>50</sub> of native drug GA against HepG2 cells after 24 h incubation was 3.26 μmol/L according to our MTT assay.



the polymeric conjugation method, by rational design and component selection, would solve many problems of insoluble chemical and natural anti-cancer agents, and at the same time achieve excellent properties of drug delivery systems.

### Acknowledgements

This work is financially supported by the 111 Project from the Ministry of Education of China and the State Administration of Foreign Expert Affairs of China (Grant No. 111-2-07), Fundamental Research Funds for the Central Universities of China (Grant No. JKY2009016, JKQ2009026, and JKP2011008), and the Natural Science Foundation of China (Grant No. 30900337).

### References

- [1] Khandare J, Minko T. *Prog Polym Sci* 2006;31:359–97.
- [2] Greenwald RB. *J Control Release* 2001;74:159–71.
- [3] Minko T. *Drug Discov Today Technologies* 2005;2:15–20.
- [4] Autherhoff H, Frauendorf H, Liesenklas W, Schwandt C. *Arch Pharm* 1962;295:833–46.
- [5] Ollis WD, Ramsay MVJ, Sutherland IO, Mongkolsuk S. *Tetrahedron* 1965;21:1453–70.
- [6] Cai SX, Jiang SC, Zhang HZ. *PCT Int Appl* 2005;51. pp. CODEN: PIXXD2 WO 2005060663 A2 20050707.
- [7] Zhao L, Guo QL, You QD, Wu ZQ, Gu HY. *Biol Pharm Bull* 2004;27:998–1003.
- [8] Liu YT, Hao K, Liu XQ, Wang GJ. *Acta Pharmacol Sin* 2006;27:1253–8.
- [9] Hao K, Liu XQ, Wang GJ, Zhao XP. *J Drug Metab Ph* 2007;32:63–8.
- [10] Dai JG, CN Patent No. 03131511.9 2003.
- [11] You QD, Guo QL, Ke X, Xiao W, Dai LL, Lin Y, CN Patent No. 03132386.3 2003.
- [12] Han JY, Xiao J, Wang H, Chang HY, Ma PS. *J Chem Ind Eng* 2001;52:64–7.
- [13] Zhu X, Zhang C, Wu XL, Tang XY, Ping QN. *Drug Dev Ind Pharm* 2008;34:2–9.
- [14] Qu GW, Zhu X, Zhang C, Ping QN. *Drug Deliv* 2009;16:363–70.
- [15] Harris JM, Zalipsky S. *Poly(ethylene glycol): chemistry and biological applications*. Plenum Press, New York, 0-306-44078-4/408.
- [16] Wang T, Wang YC, Yan LF, Wang J. *Polymer* 2009;50:5048–54.
- [17] Knop K, Hoogenboom R, Fischer D, Schubert US. *Angew Chem Int Ed* 2010;49:6288–308.
- [18] Greenwald RB, Choe YH, McGuire J, Conover CD. *Adv Drug Deliver Rev* 2003;55:217–50.
- [19] Pasut G, Veronese FM. *Prog Polym Sci* 2007;32:933–61.
- [20] Zhan FX, Chen W, Wang ZJ, Lu WT, Cheng R, Deng C, et al. *Biomacromolecules* 2011;12:3612–20.
- [21] Alani AWG, Bae Y, Rao DA, Kwon GS. *Biomaterials* 2010;31:1765–72.
- [22] Pasut G, Canal F, Via LD, Arpicco S, Veronese FM, Schiavon O. *J Control Release* 2008;127:239–48.
- [23] Greenwald RB, Pendri A, Conover C, Gilbert C, Yang R, Xia J. *J Med Chem* 1996;39:1938–40.
- [24] Cavallaro G, Pitarresi G, Licciardi M, Giammona G. *Bioconjug Chem* 2001;12:143–51.
- [25] Silva M, Ricelli NL, Seoud OE, Valentim CS, Ferreira AG, Sato DN, et al. *Arch Pharm Chem Life Sci* 2006;339:283–90.
- [26] Min T, Ye H, Zhang P, Liu J, Zhang C, Shen WB, et al. *J Appl Polym Sci* 2009;111:444–51.
- [27] Keller O, Keller WE, van Look G, Wersin G. *Org Synth* 1985;63:160–6.
- [28] Han QB, Cheung S, Tai J, Qiao CF, Song JZ, Xu HX. *Biol Pharm Bull* 2005;28:2335–7.
- [29] Liu WY, Feng F, Chen YS, You QD, Zhao SX. *Chin J Nat Med* 2004;12:75–7.
- [30] Zhang P, thesis: PEG prodrug studies on natural anti-tumor active ingredient 2008.
- [31] Greenwald RB, Pendri A, Bolikal D. *J Org Chem* 1995;60:331–6.